Palmitate induces insulin resistance in H4IIEC3 hepatocytes through reactive oxygen species produced by mitochondria.

Palmitate Induces Insulin Resistance in H4IIEC3 Hepatocytes through Reactive Oxygen Species Produced by Mitochondria

Seiji Nakamura[‡], Toshinari Takamura[‡], Naoto Matsuzawa-Nagata[§], Hiroaki Takayama[‡], Hirofumi Misu[‡], Hiroyo Noda[‡], Satoko Nabemoto[‡], Seiichiro Kurita[‡], Tsuguhito Ota[‡], Hitoshi Ando[‡], Ken-ichi Miyamoto[§], Shuichi Kaneko[‡]

[‡]Department of Disease Control and Homeostasis, Kanazawa University Graduate School of Medical Science, Kanazawa, Japan
[§]Department of Medicinal Informatics, Kanazawa University Hospital, Kanazawa, Japan

Running Title: Palmitate-induced hepatic insulin resistance

Visceral adiposity in obesity causes excessive free fatty acid (FFA) flux into the liver via the portal vein and may cause fatty liver disease and hepatic insulin resistance. However, because animal models of insulin resistance induced by lipid infusion or a high-fat diet are complex and may be accompanied by alterations not restricted to the liver, it is difficult to determine the contribution of FFAs to hepatic insulin resistance. Therefore, we treated H4IIEC3 cells, a rat hepatocyte cell line, with a monounsaturated fatty acid (oleate) and a saturated fatty acid (palmitate) to investigate the direct and initial effects of FFAs on hepatocytes. We show that palmitate, but not oleate, inhibited insulin-stimulated tyrosine phosphorylation of insulin receptor substrate 2 and serine phosphorylation of Akt, through c-Jun NH$_2$-terminal kinase (JNK) activation. Among the well-established stimuli for JNK activation, reactive oxygen species (ROS) played a causal role in palmitate-induced JNK activation. In addition, etomoxir, an inhibitor of carnitine palmitoyltransferase-1, which is the rate-limiting enzyme in mitochondrial fatty acid β-oxidation, as well as inhibitors of the mitochondrial respiratory chain complex (thenoyltrifluoroacetone and carbonyl cyanide m-chlorophenylhydrazone) decreased palmitate-induced ROS production. Together, our findings in hepatocytes indicate that palmitate inhibited insulin signal transduction through JNK activation and that accelerated β-oxidation of palmitate caused excess electron flux in the mitochondrial respiratory chain, resulting in increased ROS generation. Thus, mitochondria-derived ROS induced by palmitate may be major contributors to JNK activation and cellular insulin resistance.

1

INTRODUCTION

Insulin is the major hormone that inhibits gluconeogenesis in the liver. Visceral adiposity in obesity causes hepatic steatosis and insulin resistance. In an insulin-resistant state, impaired insulin action allows enhancement of glucose production in the liver, resulting in systemic hyperglycemia (1) and contributing to the development of type 2 diabetes. In addition, we have demonstrated experimentally that insulin resistance accelerated the pathology of steatohepatitis in genetically obese diabetic OLETF rats (2). In contrast, lipid-induced oxidative stress caused steatohepatitis and hepatic insulin resistance in mice (3). In fact, steatosis of the liver is an independent predictor of insulin resistance in patients with nonalcoholic fatty liver disease (4).

It remains unclear whether hepatic steatosis causally contributes to insulin resistance or whether it is merely a resulting pathology. Excessive dietary free fatty acid (FFA) flux into the liver via the portal vein may cause fatty liver disease and hepatic insulin resistance. Indeed, elevated plasma FFA concentrations correlate with obesity and decreased target tissue insulin sensitivity (5).

Experimentally, lipid infusion or a high-fat diet that increases circulating FFA levels promotes insulin resistance in the liver. Candidate events linking FFA to insulin resistance in vivo are the up-regulation of SREBP-1c (6), inflammation caused by activation of c-Jun amino-terminal kinase (JNK) (7) or IKKβ (8), endoplasmic reticulum (ER) stress (9), ceramide (10,11), and TRB3 (12).

However, which event is the direct and initial target of FFA in the liver is unclear. Insulin resistance induced by lipid infusion or a high-fat diet is complex and may be accompanied by alterations not restricted to the liver, making it difficult to determine the contribution of FFAs to hepatic insulin resistance. For example, hyperinsulinemia and hyperglycemia secondary to the initial event also may contribute to the development of diet-induced insulin resistance in vivo (6).

To address the early event(s) triggering the development of high-fat diet- or obesity-induced insulin resistance, we investigated the molecular mechanism(s) underlying the direct action of FFA on hepatocytes to cause insulin resistance in vitro, using the rat hepatocyte cell line H4IIEC3. We found that mitochondria-derived reactive oxygen species (ROS) were a cause of palmitate-induced insulin resistance in hepatocytes.

EXPERIMENTAL PROCEDURES

Materials—The antibody against IRS-2 was purchased from Upstate Biotechnology (Lake Placid, NY). Antibodies against phospho-tyrosine, Akt, phospho-Akt (Ser473), SAPK/JNK, phospho-SAPK/JNK (Thr183/Tyr185), and phospho-GSK-3 (Ser21/9) were purchased from Cell Signaling Technology (Beverly, MA). Antibodies against GSK-3 and phospho-c-Jun were from Santa Cruz Biotechnology (Santa Cruz, CA). Insulin from porcine pancreas, sodium palmitate, sodium oleate, myriocin, N-acetyl-L-cysteine, rotenone, TTFA, CCCP, oxypurinol, etomoxir, and tunicamycin were obtained from Sigma (St. Louis, MO). SP600125 and apocynin were from Calbiochem (La Jolla, CA). DL-a-tocopherol and H_2DCFDA were from Wako (Osaka, Japan).

Cell Culture and Fatty Acid Treatment—Studies were performed in the rat hepatoma cell line H4IIEC3, purchased from the American Type Culture Collection (Manassas, VA). Cells were cultured in DMEM (Invitrogen, Carlsbad, CA) supplemented with 10% FBS (Invitrogen), penicillin (100 U/mL), and streptomycin (0.1 mg/mL; Invitrogen). The cells were cultured at 37°C in a humidified atmosphere containing 5% CO_2, with medium changes three times a week. All studies were conducted using 80-90% confluent cells, which were treated with the indicated concentrations of FFAs in the presence of 2% FFA-free bovine serum albumin (FFA-free BSA, Sigma).

Cell Harvest and Western Blot Analysis—H4IIEC3 hepatocytes, grown to 80-90% confluency in six-well plates, were treated with the indicated reagents for 16 h in DMEM. After treatment, the cells were stimulated with insulin (1 ng/mL) for 15 min. Then, the cells were washed with ice-cold phosphate-buffered saline and lysed in buffer containing 20 mM Tris-HCl (pH 7.5), 5 mM EDTA, 1% NP-40, 2 mM Na_3VO_4, 100 mM NaF, and a protease inhibitor cocktail (Sigma). After sonication with a Bioruptor (Cosmo Bio, Tokyo, Japan), the lysates were centrifuged to remove insoluble materials. The supernatants (10 µg/lane) were separated by SDS-PAGE and transferred onto polyvinylidene difluoride membranes (Millipore, Billerica, MA). For detection of phospho-tyrosine insulin receptor and phospho-tyrosine IRS-2, the supernatants (400 µg of protein) were immunoprecipitated with a phospho-tyrosine antibody and protein G beads for 2 h at 4°C before SDS-PAGE. The membranes were blocked in a buffer containing 5% nonfat milk, 50 mM Tris (pH 7.6), 150 mM NaCl, and 0.1% Tween 20 (TBS-T) for 1 h at room temperature. They were then incubated with specific primary antibodies and subsequently with horseradish peroxidase-linked secondary antibodies. Signals were detected with a chemiluminescence detection system (ECL Plus Western blotting detection reagents; GE Healthcare Bio-Sciences, Piscataway, NJ).

Densitometric analysis was conducted directly on the blotted membrane, using a CCD camera system (LAS-3000 mini, Fuji-film, Tokyo, Japan) and Scion Image software.

Quantitative Real-time PCR—Total RNA was extracted from cultured H4IIEC3 hepatocytes using an RNeasy mini kit (Qiagen, Germantown, MD), according to the manufacturer's protocol. The cDNA was synthesized from total RNA (100 ng) using random hexamer primers, $(N)_6$, and a High Capacity cDNA Reverse Transcription kit (Applied Biosystems, Foster City, CA). Quantitative real-time PCR was performed with an ABI Prism 7900HT (Applied Biosystems). The set of specific primers and TaqMan probes in the present study were obtained from Applied Biosystems. The PCR conditions were one cycle at 50°C for 2 min and 95°C for 10 min, followed by 40 cycles at 95°C for 15 s and 60°C for 1 min.

Analysis of X-box binding protein-1 (XBP-1) mRNA Splicing—Total RNA was extracted from H4IIEC3 hepatocytes, and cDNA was synthesized as described above. The cDNA was amplified with a pair of primers (reverse 5′ CCA TGG GAA GAT GTT CTG GG 3′ and forward 5′ ACA CGC TTG GGG ATG AAT GC 3′) corresponding to the rat XBP-1 cDNA. The PCR conditions were initial denaturation at 94°C for 3 min, followed by 30 cycles of amplification (94°C for 30 s, 58°C for 30 s, 72°C for 30 s) and a final extension at 72°C for 3 min. The PCR products were separated by 2.5% agarose gel electrophoresis.

Measurement of Intracellular ROS—The intracellular formation of ROS was detected using the fluorescent probe 2′,7′-dichloro-fluorescin diacetate (H_2DCFDA), according to a published method (13). Briefly, H4IIEC3 hepatocytes, grown to 70–80% confluency in 96-well plates, were treated with the indicated reagents in DMEM for 8 h. After treatment, the cells were washed with phosphate-buffered saline, loaded with 10 μM H_2DCFDA, and incubated for 30 min at 37°C. The fluorescence was analyzed using a plate reader (Fluoroskan Ascent FL, ThermoLab Systems, Franklin, MA).

Measurement of Protein Carbonyls—The cellular concentration of proteins containing carbonyl groups (those which react with 2,4-dinitrophenylhydrazine to form the corresponding hydrazone) was determined spectrophotometrically using a protein carbonyl assay kit (Cayman Chemical, Ann Arbor, MI) according to the manufacturer's instructions and as described previously (14).

Statistical Analysis—All values are given as means ± S.E. Differences between two groups were assessed using unpaired, two-tailed t-tests. Data involving more than two groups were assessed by one-way analysis of variance (ANOVA). All calculations were performed with SPSS (version 12.0 for Windows, SPSS, Chicago, IL).

4

RESULTS

Palmitate Inhibited Insulin Receptor-Mediated Signaling—Two long-chain fatty acids were chosen for the study: palmitate, a C16:0 saturated fatty acid, and oleate, a C18:1 monounsaturated fatty acid. To examine whether FFAs impaired insulin signal transduction in H4IIEC3 hepatocytes, we assessed the effect of FFAs on insulin-stimulated tyrosine phosphorylation of IRS-2 and serine phosphorylation of Akt and GSK-3α (Fig. 1). Incubation with 0.25 mM palmitate inhibited insulin-stimulated tyrosine phosphorylation of IRS-2 by 40% in H4IIEC3 cells. Downstream of IRS-2, insulin-stimulated serine phosphorylation of Akt and GSK-3α were also inhibited by 0.25 mM palmitate treatment, by 80% and 70%, respectively, indicating an insulin-resistant state. However, the protein levels of total IRS-2, Akt, and GSK-3 were unaffected by palmitate. Furthermore, we confirmed that palmitate, but not oleate, impaired insulin-stimulated Akt serine phosphorylation in the human hepatoma cell line HepG2 (Supplemental Fig. 1).

JNK Activation by Palmitate Contributed to Palmitate-Induced Insulin Resistance—JNK, a stress-activated protein kinase, has been reported to phosphorylate IRS-1 and -2 at serine residues (15,16). Serine phosphorylation of IRSs impairs IRS tyrosine phosphorylation, leading to a reduction in insulin receptor-mediated signaling. Many studies have verified the role of JNK in fat-induced insulin resistance in several experimental systems (7,17,18). Thus, we next examined the effect of FFAs on JNK activation and its involvement in insulin signaling. Palmitate, but not oleate, dramatically increased phosphorylated JNK and c-Jun (Fig. 2). A potent and selective inhibitor of JNK, SP600125 (19), reversed the palmitate-induced phosphorylation of c-Jun (Fig. 2), suggesting that palmitate activated JNK. To test whether palmitate-induced JNK activation mediated cellular insulin resistance, we inhibited the JNK pathway with SP600125. SP600125 dose-dependently improved insulin-stimulated serine phosphorylation of Akt and GSK-3 in H4IIEC3 hepatocytes exposed to palmitate (Fig. 3). These results suggest that JNK activation by palmitate contributed to palmitate-induced insulin resistance.

Pathways for SREBP-1c and ER Stress were not Involved in Palmitate-Induced JNK Activation and Insulin Resistance in H4IIEC3 Hepatocytes—The SREBP-1c pathway has been reported to play a role in diet-induced insulin resistance in vivo. Ide et al. (6) found that high-sucrose diet-induced hyperglycemia and hyperinsulinemia up-regulated hepatic expression of SREBP-1c, leading to down-regulation of IRS-2 at the transcriptional level. However, in the present study, palmitate dramatically down-regulated the expression of SREBP-1c in H4IIEC3 hepatocytes (Supplemental Fig. 2). Consistent with this, the

mRNA (Supplemental Fig. 2) and protein (Fig. 1) levels of IRS-2 were unaffected by palmitate. Thus, palmitate itself did not appear to cause insulin resistance in hepatocytes via the SREBP-1c pathway.

ER stress is induced in insulin-resistant states such as obesity and type 2 diabetes, and in turn, this stress has been shown to lead to the inhibition of insulin signaling, through over-activation of JNK (9). As excessive FFAs have been shown to trigger ER stress in pancreatic β-cells (20), we examined whether palmitate caused ER stress in H4IIEC3 hepatocytes. ER stress induces the spliced form of XBP-1 (XBP-1s), which up-regulates the transcription of molecular chaperones, including the 78-kD glucose-regulated/binding immunoglobulin protein (GRP78) (21). Palmitate at 0.25 mM did not alter the expression level of GRP78 mRNA or the splicing pattern of XBP-1, unlike tunicamycin, an agent commonly used to induce ER stress (Supplemental Fig. 3). Next, we compared the impact of palmitate and tunicamycin on insulin-stimulated signal transduction and JNK activation (Supplemental Fig. 4). The inhibitory effect of tunicamycin on insulin-stimulated serine phosphorylation of Akt was mild and not significant, compared with that of palmitate. Additionally, the increment in phosphorylated JNK by tunicamycin was lower and not significant compared with that of palmitate. These results suggest that ER stress played a minor role in palmitate-induced JNK activation and cellular insulin resistance in H4IIEC3 hepatocytes.

Palmitate Induced Reactive Oxygen Species (ROS) Production—In addition to ER stress, increased cellular ROS levels are known to stimulate threonine phosphorylation of JNK (22). Indeed, ROS levels are increased in clinical conditions associated with insulin resistance, such as sepsis, burn injuries, obesity, and type 2 diabetes (23). Furthermore, FFAs have been reported to generate ROS in various cells such as pancreatic islet cells (24), cardiac myocytes (25), and adipocytes (23).

Thus, we hypothesized that palmitate increased intracellular ROS production and thereby activated JNK, leading to the impaired insulin signaling. To evaluate this, H4IIEC3 hepatocytes were incubated with H_2DCFDA, a fluorescent probe, to visualize intracellular ROS, with or without palmitate. H_2DCFDA-associated fluorescence was elevated by 58% after incubation with 0.25 mM palmitate for 8 h, and palmitate induced more ROS production than oleate (Fig. 4). Consistent with this, the amount of protein carbonyls, a marker of oxidative stress, significantly increased in palmitate-treated hepatocytes (4.6 ± 0.5 nmol/mg protein), compared with control cells (3.1 ± 0.4 nmol/mg protein). These results suggest that FFAs, especially palmitate, can cause ROS production and oxidative stress in H4IIEC3 hepatocytes.

Anti-oxidants Prevented Palmitate-Induced Insulin Resistance—We next sought to test

whether palmitate-induced ROS overproduction had a causal role in insulin resistance by assessing whether two anti-oxidant reagents, N-acetyl-L-cysteine (NAC) and α-tocopherol, could also act as insulin sensitizers. NAC and α-tocopherol dose-dependently suppressed palmitate-induced intracellular ROS production; NAC at 10 mM and α-tocopherol at 0.4 mM suppressed ROS production by 50% and 60%, respectively (Fig. 5). In parallel with decreased ROS levels, the anti-oxidants recovered the insulin-stimulated Akt phosphorylation impaired by palmitate; NAC at 10 mM and α-tocopherol at 0.4 mM recovered the phosphorylation by 40% and 35%, respectively (Fig. 6). Furthermore, these anti-oxidants suppressed palmitate-induced JNK phosphorylation; NAC at 10 mM and α-tocopherol at 0.4 mM suppressed it by 80% and 55%, respectively (Fig. 7). These results suggest that palmitate increased ROS levels in H4IIEC3 hepatocytes and thereby activated JNK, resulting in insulin resistance.

Palmitate Induced ROS Overproduction in Mitochondria—To define the source of ROS induced by palmitate in H4IIEC3 hepatocytes, we examined the cellular pathway involved in ROS production, including NADPH oxidase, xanthine oxidase, and mitochondria-mediated pathways. Palmitate-induced ROS production was markedly suppressed by rotenone, an inhibitor of mitochondrial respiratory chain complex I; thenoyltrifluoroacetone (TTFA), an inhibitor of mitochondrial respiratory chain complex II; and carbonyl cyanide *m*-chlorophenylhydrazone (CCCP), an uncoupler of oxidative phosphorylation (Fig. 8). In contrast, ROS production in palmitate-treated H4IIEC3 cells was not suppressed by apocynin, an inhibitor of NADPH oxidase, or oxypurinol, an inhibitor of xanthine oxidase. These results suggest that the mitochondrial respiratory chain is involved in palmitate-induced ROS overproduction in H4IIEC3 hepatocytes.

Palmitate Increased ROS through the Mitochondrial Fatty Acid β-oxidation-Respiratory Chain—FFAs are metabolized in the mitochondrial fatty acid β-oxidation pathway, which supplies the mitochondrial respiratory chain with electrons. Large amounts of electrons entering the respiratory chain may cause abnormal reduction of oxygen, leading to ROS production. Thus, we next examined whether palmitate-induced ROS production was dependent on mitochondrial fatty acid β-oxidation. Carnitine palmitoyltransferase-1a (CPT-1a) is the rate-limiting enzyme in mitochondrial fatty acid β-oxidation. As expected, etomoxir, a CPT-1 inhibitor, decreased palmitate-induced ROS production, by 80% (Fig. 9A). Furthermore, palmitate, but not oleate, significantly increased expression of the *CPT-1a* gene (Fig. 9B). This up-regulation may contribute to palmitate-induced ROS overproduction, because the accelerated β-oxidation should cause excessive electron flux in the respiratory chain.

DISCUSSION

In the present study, we investigated the direct action of fatty acids on insulin signaling in hepatocytes. The saturated fatty acid palmitate, but not the unsaturated fatty acid oleate, impaired insulin-induced tyrosine phosphorylation of IRS-2, serine phosphorylation of Akt, and serine phosphorylation of GSK-3α, all of which are indicative of insulin resistance in cultured H4IIEC3 hepatocytes. Unlike in vivo findings (6), the expression of the *SREBP-1c* gene was down-regulated by adding palmitate to cultured H4IIEC3 hepatocytes, which is likely a result of a negative feedback loop for fatty acid synthesis, and IRS-2 protein levels were unaffected. FFA-induced insulin resistance has been reported in other insulin-sensitive cells such as adipocytes (18) and skeletal muscle cells (26). These studies, together with the present results, suggest that FFA inhibits insulin signaling at the level of tyrosine phosphorylation of IRSs, regardless of cell type. Similar to the findings in 3T3-L1 adipocytes (18) and primary mouse hepatocytes and pancreatic β-cells (16), the activation of JNK, a known suppressor of the tyrosine phosphorylation of IRSs, was involved in FFA-induced tyrosine phosphorylation of IRS-2 in cultured H4IIEC3 hepatocytes. Because a JNK inhibitor, SP600125, largely restored palmitate-induced impairment of the insulin signaling pathway, JNK activation seems to play a major role in the development of palmitate-induced insulin resistance in H4IIEC3

hepatocytes. Our results support in vivo finding that JNK is activated in the liver of an animal model of obesity and diabetes in which FFA influx into the liver is elevated (9,27). The overexpression of JNK in mouse liver resulted in hepatic insulin resistance at the level of IRS tyrosine phosphorylation, and the overexpression of a dominant negative mutant of JNK in the liver accelerated hepatic insulin signaling (17).

Given that JNK is activated by many types of cellular stresses (28), we next searched for a link between palmitate treatment and JNK activation in H4IIEC3 hepatocytes. ER stress was unlikely to mediate palmitate-induced insulin resistance in H4IIEC3 hepatocytes, because palmitate caused insulin resistance independent of ER stress, whereas tunicamycin caused ER stress without affecting insulin action. Instead, we found that palmitate-induced ROS generation mediated insulin resistance. ROS are one of many factors suggested to have a possible role in insulin resistance (29,30). ROS include reactive products such as superoxide anion, hydrogen peroxide, and hydroxyl radical, which are formed as by-products of mitochondrial oxidative phosphorylation (OXPHOS). Thus, as a rule, increased mitochondrial OXPHOS flux leads to increased formation of ROS (31,32). ROS can also be produced during β-oxidation of fatty acids, especially as a by-product of peroxisomal acyl-CoA oxidase activity (32). Additionally, ROS can be produced by dedicated enzymes such as NADPH oxidase (33) present in

phagocytic cells, where ROS are an important part of cellular defense mechanisms. Using specific inhibitors of subcellular ROS, we identified mitochondrial OXPHOS as an important source of palmitate-induced ROS generation in H4IIEC3 hepatocytes. FFAs supply mitochondrial OXPHOS with electrons through mitochondrial fatty acid β-oxidation. A final metabolite of fatty acids, acetyl-CoA, is metabolized in the TCA cycle. In the processes of fatty acid β-oxidation and the TCA cycle, NADH and $FADH_2$ are generated and could supply excessive electrons for OXPHOS.

NAC, a scavenger of ROS, dose-dependently restored glutathione in palmitate-treated cells (Supplemental Fig. 5). However, glutathione restoration by NAC was unable to completely rescue palmitate-induced insulin resistance. Furthermore, the combination of NAC and alpha-tocopherol did not completely reverse JNK activation (Supplemental Fig. 6A and 6B) and only partly rescued palmitate-induced insulin resistance (Supplemental Fig. 7A and 7B). Therefore, other mechanisms may also be involved in insulin resistance caused by palmitate.

De novo ceramide synthesis is a potential pathway contributing to palmitate-induced JNK activation. Ceramide derived from saturated fatty acids has been reported to activate JNK and inhibit insulin-induced Akt phosphorylation in myocytes (34–36). In our investigation, palmitate increased the intracellular content of ceramide in

H4IIEC3 hepatocytes (Supplemental Fig 8). Unfortunately, even at the maximum myriosin concentration, the intracellular accumulation of ceramide was not blocked by myriosin, a potent inhibitor of serine palmitoyltransferase at the first step in ceramide biosynthesis, (Supplemental Fig. 8). Furthermore, ceramide accumulation was not blocked when myriosin was used in combination with fumonisin B1, an inhibitor of ceramide synthase (data not shown). Therefore, we cannot rule out the possibility that intracellular ceramide contributes to palmitate-induced insulin resistance in H4IIEC3 hepatocytes. Further studies are required to assess the role of the ceramide pathway in palmitate-induced insulin resistance in hepatocytes.

In the present study, etomoxir, an inhibitor of CPT-1, decreased palmitate-induced intracellular ROS production. Additionally, palmitate, but not oleate, significantly increased the expression of the CPT-1a gene, which may account for the observed differences in insulin action between palmitate and oleate.

Recently, it was reported that fatty acid composition may be a determinant in insulin sensitivity (37,38). In this regard, we investigated the effect of oleate on insulin signaling in palmitate-treated hepatocytes. Surprisingly, oleate dose-dependently reversed palmitate-induced ROS generation, JNK phosphorylation, and rescued palmitate-induced phosphorylation of Akt (Takayama and

10

Takamura, unpublished data). Further investigations aimed at elucidating the molecular basis underlying the differential roles and interactions of FFAs are required.

In conclusion, this study identified mitochondrial ROS generation as a critical factor in palmitate-induced hepatic insulin resistance. Palmitate may induce CPT-1 expression, accelerate metabolism, supply excess electrons for mitochondrial OXPHOS, and generate ROS. ROS then desensitize the insulin signaling pathway by activating JNK, impairing tyrosine phosphorylation of IRS-2, and causing hepatic insulin resistance. The results suggest that an initial event in high-fat/sucrose diet-induced or obesity-induced insulin resistance in the liver is mitochondrial ROS generation, which could potentially be a therapeutic target. In addition to previously suggested JNK inhibitors or anti-oxidants, mitochondrial uncouplers such as CCCP may provide a candidate therapeutic strategy for this pathway, by preventing ROS generation.

REFERENCES

1. Saltiel, A. R., and Kahn, C. R. (2001) *Nature* **414**, 799-806

2. Ota, T., Takamura, T., Kurita, S., Matsuzawa, N., Kita, Y., Uno, M., Akahori, H., Misu, H., Sakurai, M., Zen, Y., Nakanuma, Y., and Kaneko, S. (2007) *Gastroenterology* **132**, 282-293

3. Matsuzawa, N., Takamura, T., Kurita, S., Misu, H., Ota, T., Ando, H., Yokoyama, M., Honda, M., Zen, Y., Nakanuma, Y., Miyamoto, K., and Kaneko, S. (2007) *Hepatology* **46**, 1392-1403

4. Sakurai, M., Takamura, T., Ota, T., Ando, H., Akahori, H., Kaji, K., Sasaki, M., Nakanuma, Y., Miura, K., and Kaneko, S. (2007) *J Gastroenterol* **42**, 312-317

5. Boden, G. (1997) *Diabetes* **46**, 3-10

6. Ide, T., Shimano, H., Yahagi, N., Matsuzaka, T., Nakakuki, M., Yamamoto, T., Nakagawa, Y., Takahashi, A., Suzuki, H., Sone, H., Toyoshima, H., Fukamizu, A., and Yamada, N. (2004) *Nat Cell Biol* **6**, 351-357

7. Hirosumi, J., Tuncman, G., Chang, L., Gorgun, C. Z., Uysal, K. T., Maeda, K., Karin, M., and Hotamisligil, G. S. (2002) *Nature* **420**, 333-336

8. Boden, G., She, P., Mozzoli, M., Cheung, P., Gumireddy, K., Reddy, P., Xiang, X., Luo, Z., and Ruderman, N. (2005) *Diabetes* **54**, 3458-3465

9. Ozcan, U., Cao, Q., Yilmaz, E., Lee, A. H., Iwakoshi, N. N., Ozdelen, E., Tuncman, G., Gorgun, C., Glimcher, L. H., and Hotamisligil, G. S. (2004) *Science* **306**, 457-461

10. Kim, J. K., Fillmore, J. J., Chen, Y., Yu, C., Moore, I. K., Pypaert, M., Lutz, E. P., Kako, Y., Velez-Carrasco, W., Goldberg, I. J., Breslow, J. L., and Shulman, G. I. (2001) *Proc Natl Acad Sci U S A* **98**, 7522-7527

11. Turinsky, J., O'Sullivan, D. M., and Bayly, B. P. (1990) *J Biol Chem* **265**, 16880-16885

12. Du, K., Herzig, S., Kulkarni, R. N., and Montminy, M. (2003) *Science* **300**, 1574-1577

13. Nishikawa, T., Edelstein, D., Du, X. L., Yamagishi, S., Matsumura, T., Kaneda, Y., Yorek, M. A., Beebe, D., Oates, P. J., Hammes, H. P., Giardino, I., and Brownlee, M. (2000) *Nature* **404**, 787-790

14. Matsuzawa-Nagata, N., Takamura, T., Ando, H., Nakamura, S., Kurita, S., Misu, H., Ota, T., Yokoyama, M., Honda, M., Miyamoto, K., and Kaneko, S. (2008) *Metabolism* **57**, 1071-1077

15. Aguirre, V., Uchida, T., Yenush, L., Davis, R., and White, M. F. (2000) *J Biol Chem* **275**, 9047-9054

12

16. Solinas, G., Naugler, W., Galimi, F., Lee, M. S., and Karin, M. (2006) *Proc Natl Acad Sci U S A* **103**, 16454-16459

17. Nakatani, Y., Kaneto, H., Kawamori, D., Hatazaki, M., Miyatsuka, T., Matsuoka, T. A., Kajimoto, Y., Matsuhisa, M., Yamasaki, Y., and Hori, M. (2004) *J Biol Chem* **279**, 45803-45809

18. Nguyen, M. T., Satoh, H., Favelyukis, S., Babendure, J. L., Imamura, T., Sbodio, J. I., Zalevsky, J., Dahiyat, B. I., Chi, N. W., and Olefsky, J. M. (2005) *J Biol Chem* **280**, 35361-35371

19. Bennett, B. L., Sasaki, D. T., Murray, B. W., O'Leary, E. C., Sakata, S. T., Xu, W., Leisten, J. C., Motiwala, A., Pierce, S., Satoh, Y., Bhagwat, S. S., Manning, A. M., and Anderson, D. W. (2001) *Proc Natl Acad Sci U S A* **98**, 13681-13686

20. Karaskov, E., Scott, C., Zhang, L., Teodoro, T., Ravazzola, M., and Volchuk, A. (2006) *Endocrinology* **147**, 3398-3407

21. Harding, H. P., Calfon, M., Urano, F., Novoa, I., and Ron, D. (2002) *Annu Rev Cell Dev Biol* **18**, 575-599

22. Kaneto, H., Kawamori, D., Nakatani, Y., Gorogawa, S., and Matsuoka, T. A. (2004) *Drug News Perspect* **17**, 447-453

23. Furukawa, S., Fujita, T., Shimabukuro, M., Iwaki, M., Yamada, Y., Nakajima, Y., Nakayama, O., Makishima, M., Matsuda, M., and Shimomura, I. (2004) *J Clin Invest* **114**, 1752-1761

24. Carlsson, C., Borg, L. A., and Welsh, N. (1999) *Endocrinology* **140**, 3422-3428

25. Miller, T. A., LeBrasseur, N. K., Cote, G. M., Trucillo, M. P., Pimentel, D. R., Ido, Y., Ruderman, N. B., and Sawyer, D. B. (2005) *Biochem Biophys Res Commun* **336**, 309-315

26. Chavez, J. A., and Summers, S. A. (2003) *Arch Biochem Biophys* **419**, 101-109

27. Nakatani, Y., Kaneto, H., Kawamori, D., Yoshiuchi, K., Hatazaki, M., Matsuoka, T. A., Ozawa, K., Ogawa, S., Hori, M., Yamasaki, Y., and Matsuhisa, M. (2005) *J Biol Chem* **280**, 847-851

28. Davis, R. J. (2000) *Cell* **103**, 239-252

29. Evans, J. L., Goldfine, I. D., Maddux, B. A., and Grodsky, G. M. (2002) *Endocr Rev* **23**, 599-622

30. Houstis, N., Rosen, E. D., and Lander, E. S. (2006) *Nature* **440**, 944-948

31. Brownlee, M. (2001) *Nature* **414**, 813-820

32. Osmundsen, H., Bremer, J., and Pedersen, J. I. (1991) *Biochim Biophys Acta* **1085**,

13

141-158

33. De Minicis, S., Bataller, R., and Brenner, D. A. (2006) *Gastroenterology* **131**, 272-275

34. Chavez, J. A., Knotts, T. A., Wang, L. P., Li, G., Dobrowsky, R. T., Florant, G. L., and Summers, S. A. (2003) *J Biol Chem* **278**, 10297-10303

35. Powell, D. J., Turban, S., Gray, A., Hajduch, E., and Hundal, H. S. (2004) *Biochem J* **382**, 619-629

36. Schmitz-Peiffer, C., Craig, D. L., and Biden, T. J. (1999) *J Biol Chem* **274**, 24202-24210

37. Bruce, C. R., and Febbraio, M. A. (2007) *Nat Med* **13**, 1137-1138

38. Cao, H., Gerhold, K., Mayers, J. R., Wiest, M. M., Watkins, S. M., and Hotamisligil, G. S. (2008) *Cell* **134**, 933-944

Abbreviations used are: IRS, insulin receptor substrate; FFA, free fatty acid; GSK, glycogen synthase kinase; JNK, c-Jun NH_2-terminal kinase; ER, endoplasmic reticulum; GRP, glucose-regulated protein; XBP, X-box binding protein; ROS, reactive oxygen species; NAC, N-acetyl-L-cysteine; TTFA, 2-thenoyltrifluoroacetone; CCCP, carbonyl cyanide 3-chlorophenylhydrazone.

FIGURE LEGENDS

FIGURE 1. Effects of palmitate and oleate on insulin-stimulated tyrosine phosphorylation of IRS-2 and serine phosphorylation of Akt and GSK-3 in H4IIEC3 hepatocytes. (A) H4IIEC3 cells were incubated in the presence or absence of palmitate (Pal) or oleate (Ole) for 16 h prior to stimulation with insulin (1 ng/mL, 15 min). Total cell lysates were resolved by SDS-PAGE, transferred to a PVDF membrane, and immunoblotted with the indicated antibodies. Total cell lysates were subjected to immunoprecipitation with phosphotyrosine antibody prior to SDS-PAGE to examine tyrosine phosphorylation of IRS-2. Detection was by enhanced chemiluminescence. Representative blots are shown. (B) The values from densitometry of three (p-IRS-2), eight (p-Akt), or five (p-GSK-3α) independent experiments were normalized to the level of total IRS-2, Akt, or GSK-3α protein, respectively, and expressed as the mean fold increase over control ± S.E. * $p < 0.05$, versus insulin treatment alone. ** $p < 0.01$, versus insulin treatment alone.

FIGURE 2. Effects of palmitate and oleate on JNK activation in H4IIEC3 hepatocytes. (A) H4IIEC3 cells were incubated in the presence or absence of FFAs [palmitate (Pal) or oleate (Ole)] and the JNK inhibitor SP600125 (SP) for 16 h. Total cell lysates were resolved by SDS-PAGE, transferred to a PVDF membrane, and immunoblotted with the indicated antibodies. Detection was by enhanced chemiluminescence. Representative blots are shown. (B) The values from densitometry of four (p-JNK) independent experiments were normalized to the level of total

JNK (p-c-Jun was not normalized; n = 4) and expressed as the mean fold increase over control ± S.E. ** $p < 0.01$, versus control. †† $p < 0.01$, versus palmitate treatment.

FIGURE 3. Effect of a JNK inhibitor on palmitate-induced alterations in insulin-stimulated phosphorylation of Akt and GSK-3 in H4IIEC3 hepatocytes. (A) H4IIEC3 cells were incubated in the presence or absence of palmitate (Pal) and the JNK inhibitor SP600125 (SP) for 16 h prior to stimulation with insulin (1 ng/mL, 15 min). Total cell lysates were resolved by SDS-PAGE, transferred to a PVDF membrane, and immunoblotted with the indicated antibodies. Detection was by enhanced chemiluminescence. Representative blots are shown. (B) The values from densitometry of four (p-Akt or p-GSK-3) independent experiments were normalized to the level of total Akt or GSK-3 protein, respectively, and expressed as the mean fold increase over control ± S.E. ** $p < 0.01$, versus palmitate treatment.

FIGURE 4. Effect of palmitate on oxidative stress in H4IIEC3 hepatocytes. H4IIEC3 cells were incubated in the presence or absence of palmitate (Pal) or oleate (Ole) for 8 h. Intracellular ROS production was quantified using the fluorescent probe H_2DCFDA. The values are expressed as mean fold increase over control ± S.E. (n = 4). ** $p < 0.01$, versus control. †† $p < 0.01$, versus 0.25 mM palmitate treatment.

FIGURE 5. Effects of anti-oxidants on palmitate-induced intracellular ROS production in H4IIEC3 hepatocytes. H4IIEC3 cells were incubated in the presence or absence of palmitate (Pal) and anti-oxidants for 8 h. Intracellular ROS production was quantified using the fluorescent probe H_2DCFDA. The values are expressed as mean fold increase over control ± S.E. (n = 4). * $p < 0.05$, versus palmitate treatment alone. ** $p < 0.01$, versus palmitate treatment alone. NAC, N-acetyl-L-cysteine; Toc, α-tocopherol.

FIGURE 6. Effects of anti-oxidants on palmitate-induced alterations in insulin-stimulated serine phosphorylation of Akt in H4IIEC3 hepatocytes. (A) H4IIEC3 cells were incubated in the presence or absence of palmitate (Pal) and anti-oxidants for 16 h prior to stimulation with insulin (1ng/mL, 15 min). Total cell lysates were resolved by SDS-PAGE, transferred to a PVDF membrane, and immunoblotted with the indicated antibodies. Detection was by enhanced chemiluminescence. Representative blots are shown. (B) The values from densitometry of four (NAC) or five (α-tocopherol) independent experiments were normalized to the level of total Akt

16

protein and expressed as the mean fold increase over control ± S.E. * $p < 0.05$, versus palmitate treatment. NAC, N-acetyl-L-cysteine; Toc, α-tocopherol.

FIGURE 7. Effects of anti-oxidants on palmitate-induced JNK activation in H4IIEC3 hepatocytes. (A) H4IIEC3 cells were incubated in the presence or absence of palmitate (Pal) and anti-oxidants for 16 h. Total cell lysates were resolved by SDS-PAGE, transferred to a PVDF membrane, and immunoblotted with the indicated antibodies. Detection was by enhanced chemiluminescence. Representative blots are shown. (B) The values from densitometry of four (NAC or α-tocopherol) independent experiments were normalized to the level of total JNK protein and expressed as the mean fold increase over control ± S.E. ** $p < 0.01$, versus palmitate treatment alone. NAC, N-acetyl-L-cysteine; Toc, α-tocopherol

FIGURE 8. Effects of ROS-producing pathway inhibitors on palmitate-induced ROS production in H4IIEC3 hepatocytes. H4IIEC3 cells were incubated in the presence or absence of palmitate (Pal) and each ROS-producing pathway inhibitor for 8 h. Intracellular ROS production was quantified using the fluorescent probe H$_2$DCFDA. The values are expressed as mean fold increase over control ± S.E. (n = 4). * $p < 0.05$, versus palmitate treatment alone. ** $p < 0.01$, versus palmitate treatment alone. Rot, rotenone; Apo, apocynin; Oxy, oxypurinol

FIGURE 9. Involvement of mitochondrial fatty acid oxidation in palmitate-induced ROS production. (A) H4IIEC3 cells were incubated in the presence or absence of palmitate (Pal) and the CPT-1 inhibitor etomoxir (Eto) for 8 h. Intracellular ROS production was quantified using the fluorescent probe H$_2$DCFDA. The values are expressed as mean fold increase over control ± S.E. (n = 4). (B) H4IIEC3 cells were incubated in the presence or absence of palmitate (Pal) or oleate (Ole) for 16 h. Total RNA was extracted and subjected to reverse transcription. Using the cDNA as a template, the amounts of CPT-1 mRNA were detected by real-time PCR. The values were normalized to the level of 18S ribosomal RNA and expressed as mean fold increase over control ± S.E. (n = 3). * $p < 0.05$, versus control. ** $p < 0.01$, versus palmitate treatment alone.

FIGURE 10. Proposed model for palmitate-induced hepatic insulin resistance.
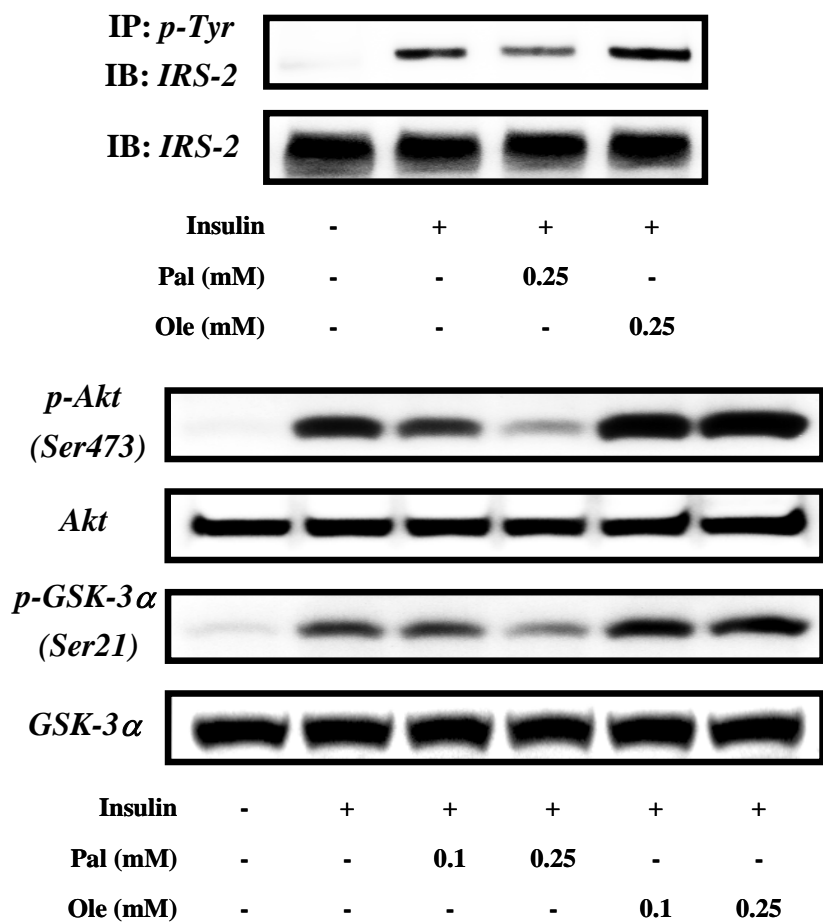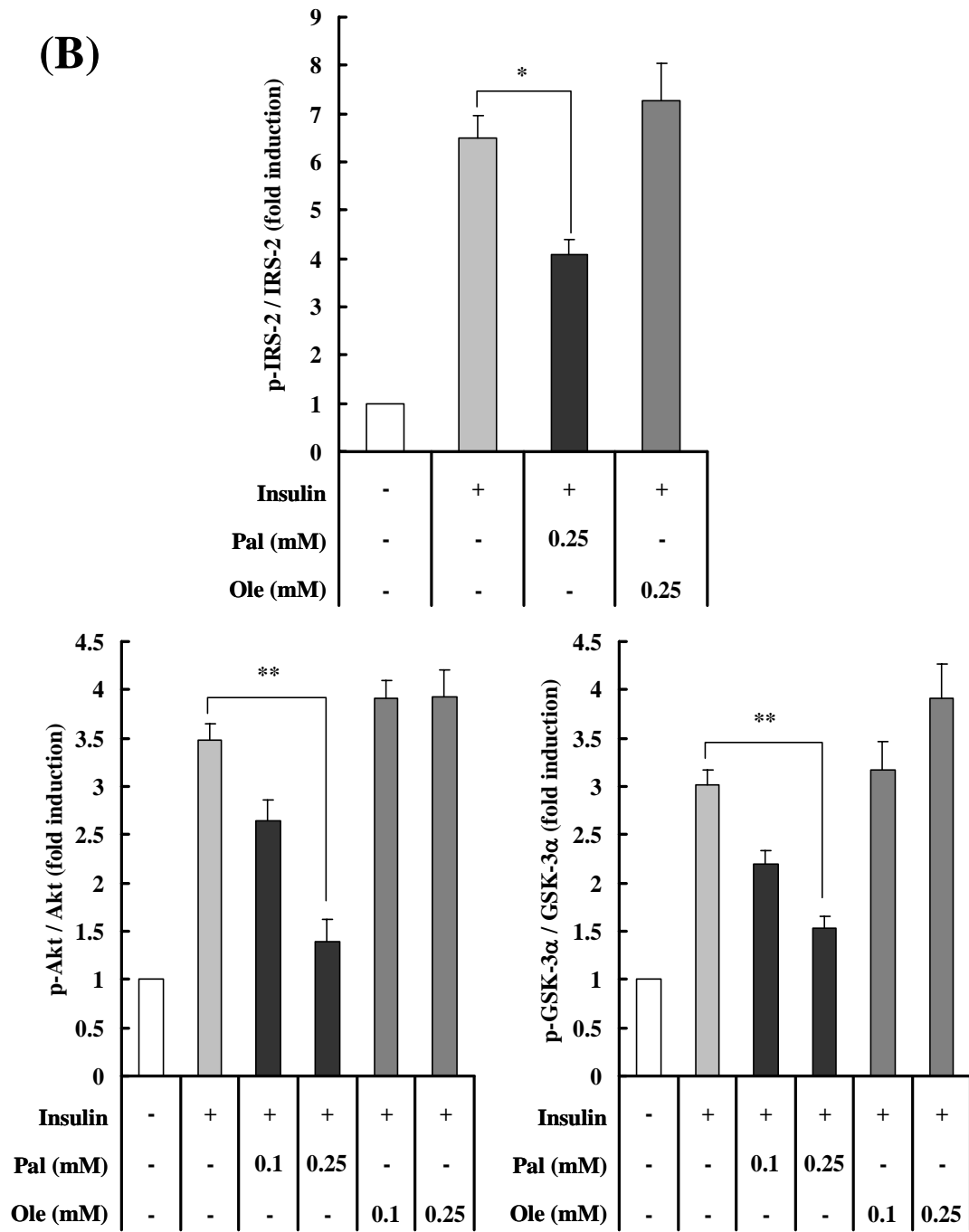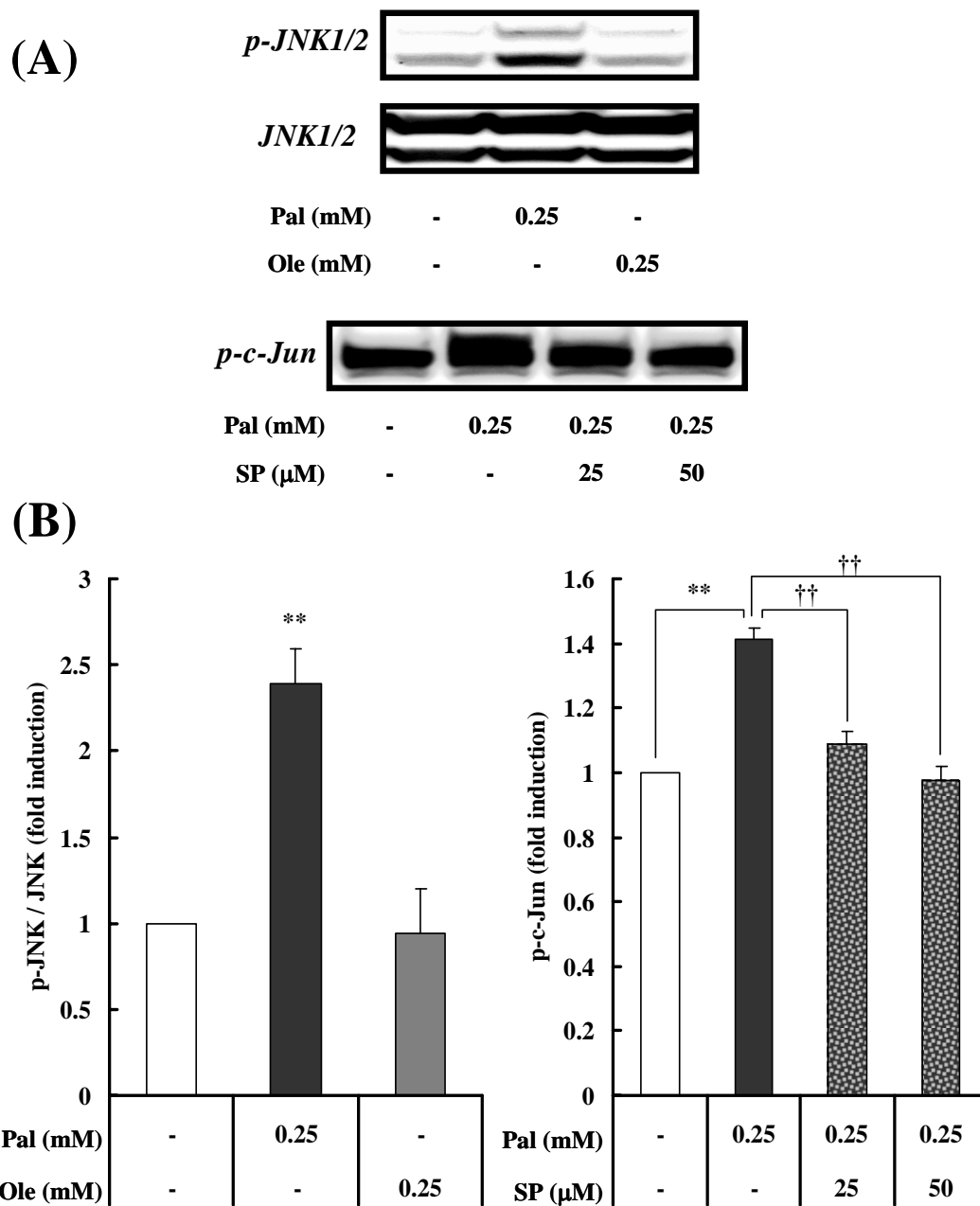
17

Figure 1

(A)

Insulin	-	+	+	+
Pal (mM)	-	-	0.25	-
Ole (mM)	-	-	-	0.25

Insulin	-	+	+	+	+	+
Pal (mM)	-	-	0.1	0.25	-	-
Ole (mM)	-	-	-	-	0.1	0.25

18

Figure 1

Figure 2

(A)

Pal (mM)	-	0.25	-
Ole (mM)	-	-	0.25

Pal (mM)	-	0.25	0.25	0.25
SP (µM)	-	-	25	50

(B)

Figure 3

(A)

	Insulin	-	+	+	+	+
	Pal (mM)	-	-	0.25	0.25	0.25
	SP (µM)	-	-	-	25	50

(B)

Figure 4

Figure 5

	-	0.25	0.25	0.25	0.25	0.25
Pal (mM)	-	0.25	0.25	0.25	0.25	0.25
NAC (mM)	-	-	5	10	-	-
Toc (mM)	-	-	-	-	0.2	0.4

23

Figure 6

Figure 7

(A)

(B)

Figure 8

| Pal (mM) | - | 0.25 | 0.25 | 0.25 | 0.25 | 0.25 | 0.25 |
| ROS inhibitor | - | - | Rot | TTFA | CCCP | Apo | Oxy |

Figure 9

(A)

| Pal (mM) | - | 0.25 | 0.25 |
| Inhibitor | - | - | Eto |

(B)

| Pal (mM) | - | 0.25 | - |
| Ole (mM) | - | - | 0.25 |

Figure 10

[Liver]

IR

IRS

P

JNK

P

P

Akt

P

Insulin action

ROS

Hepatic insulin resistance

[Adipose tissue]
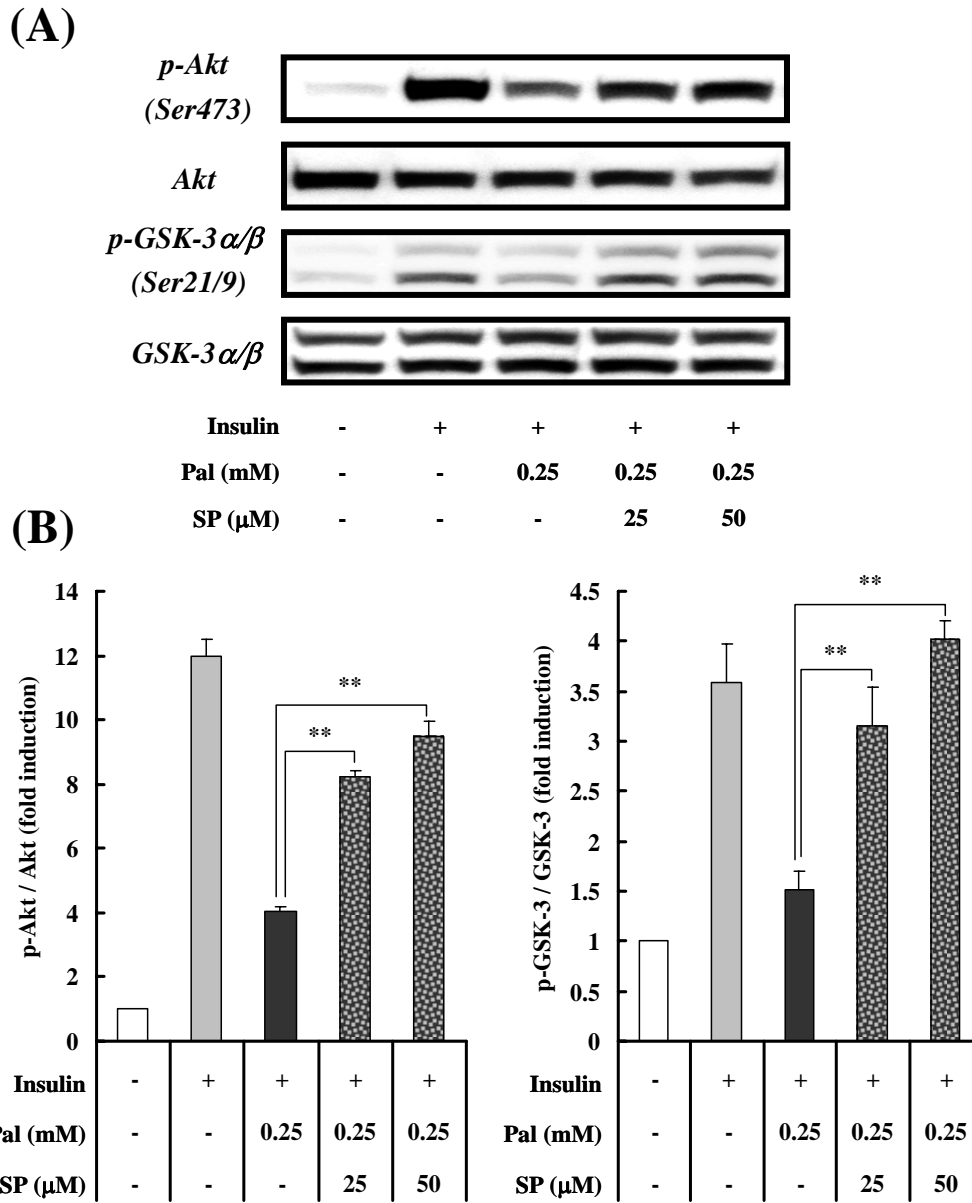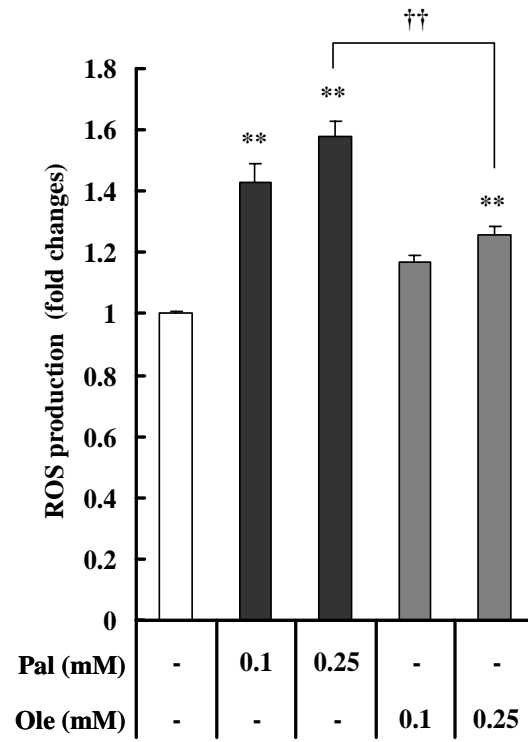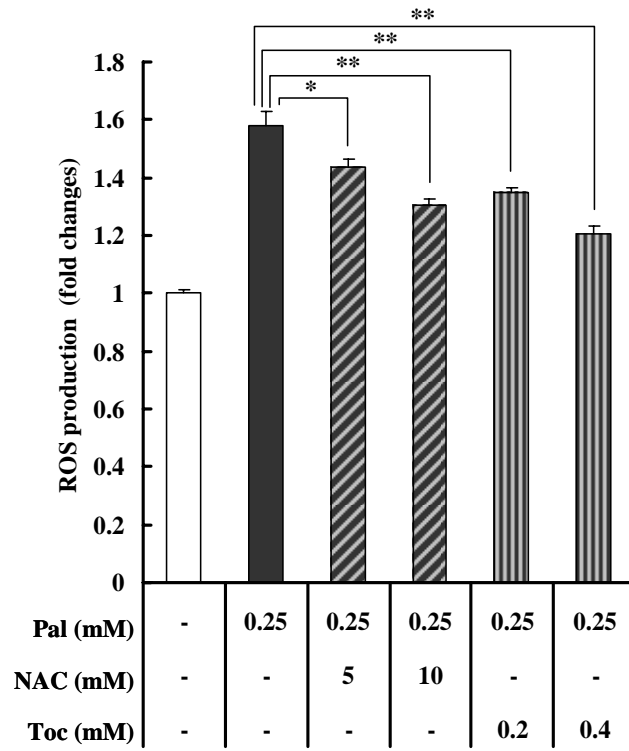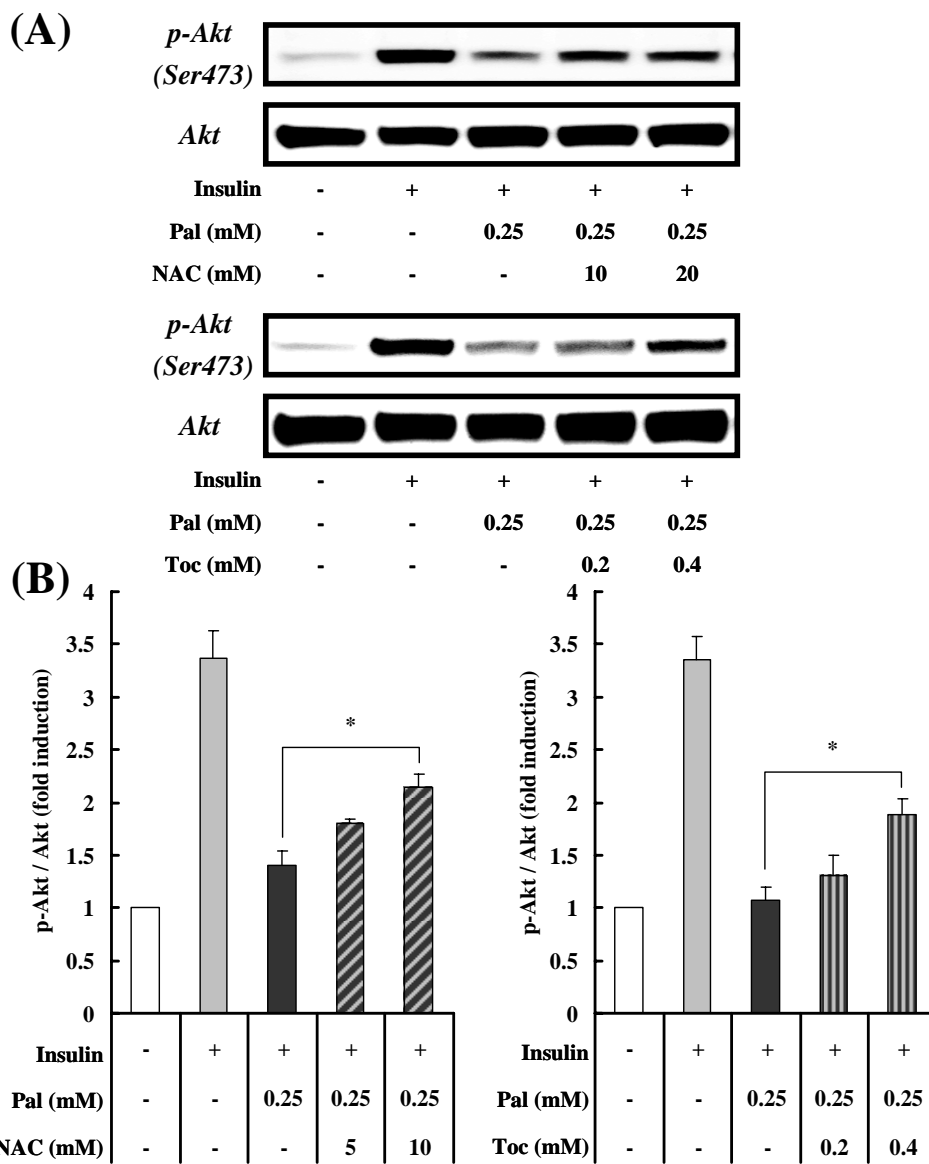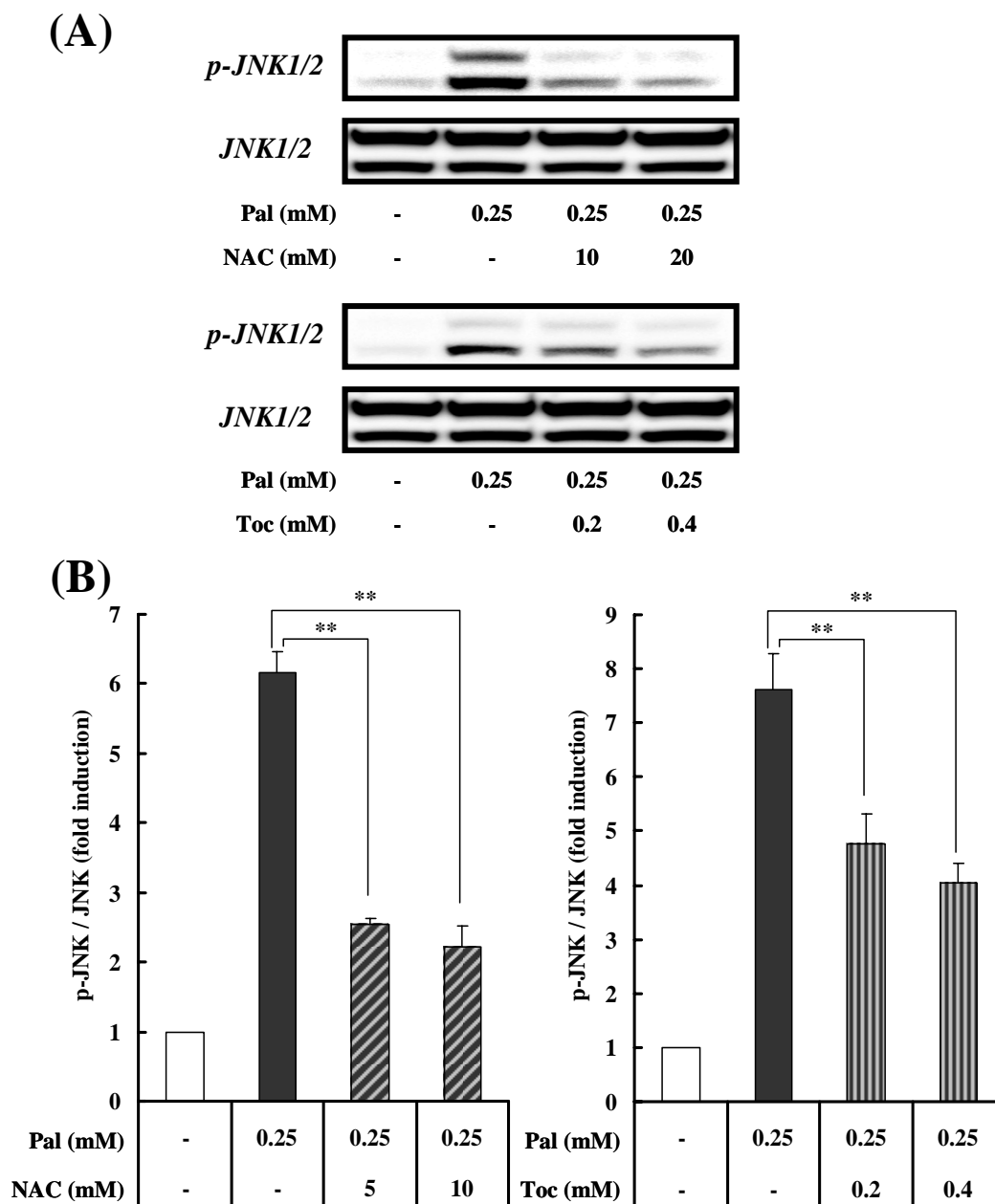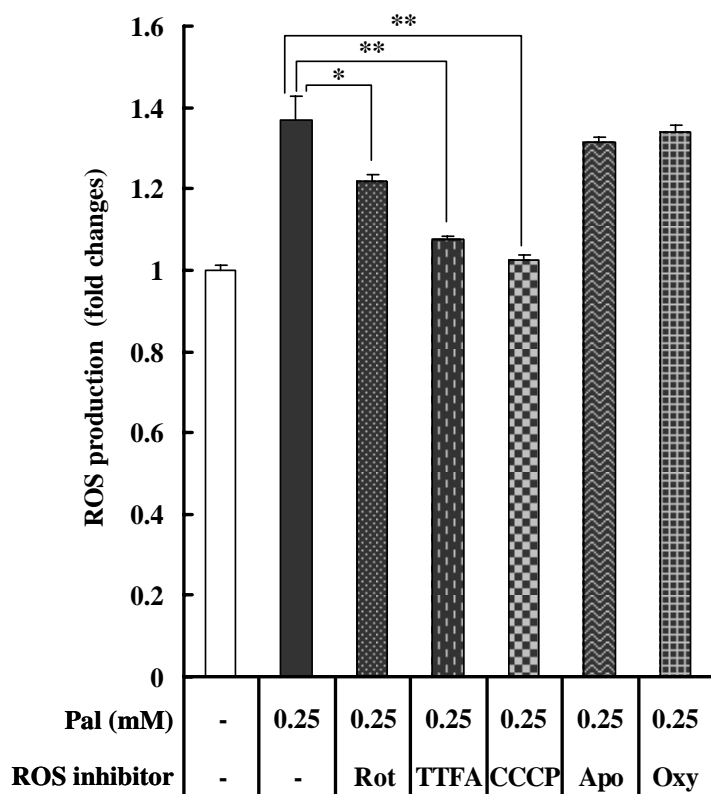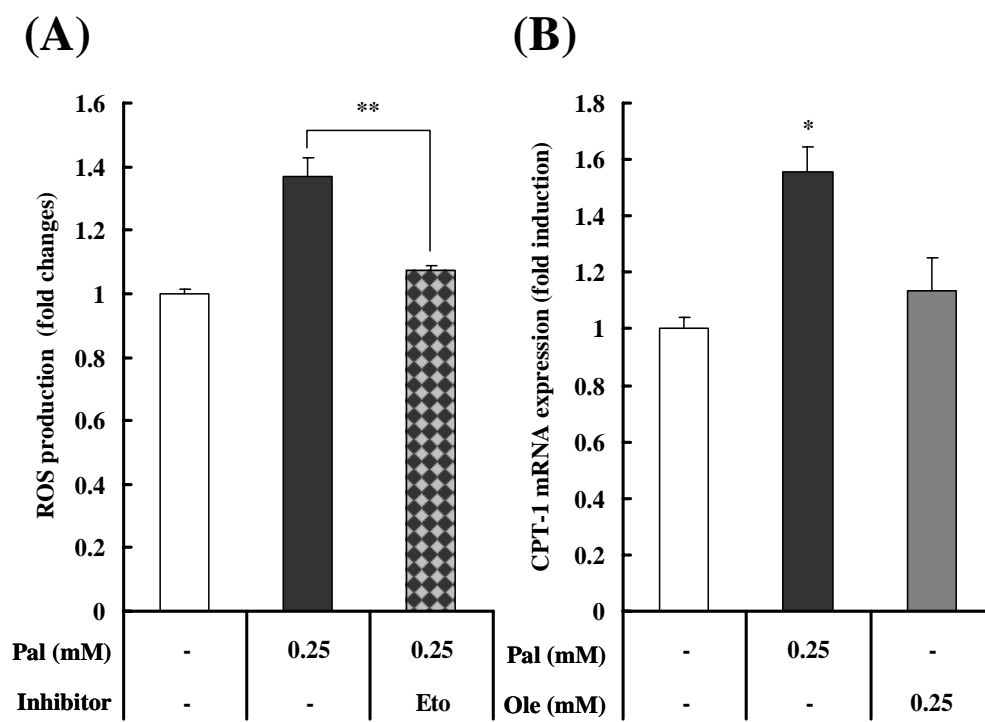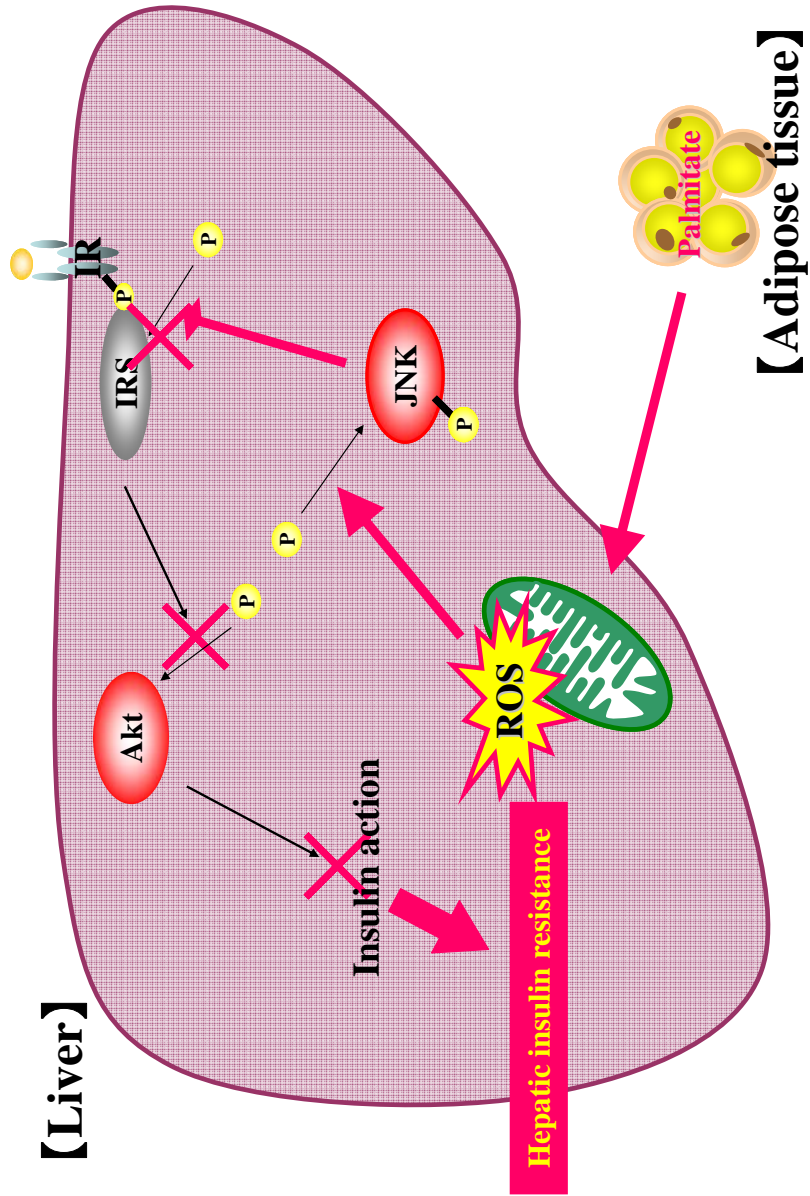
Palmitate

Supplemental Fig. 1. Effects of palmitate and oleate on insulin-stimulated serine phosphorylation of Akt in HepG2 cells. HepG2 cells were incubated in the presence or absence of FFAs *A*, palmitate (Pal); *B*, oleate (Ole)] for 16 h prior to stimulation with insulin (1 ng/mL, 15 min). Total cell lysates were resolved by SDS-PAGE, transferred to a PVDF membrane, and immunoblotted with the indicated antibodies. Detection was by enhanced chemiluminescence. Representative blots are shown.
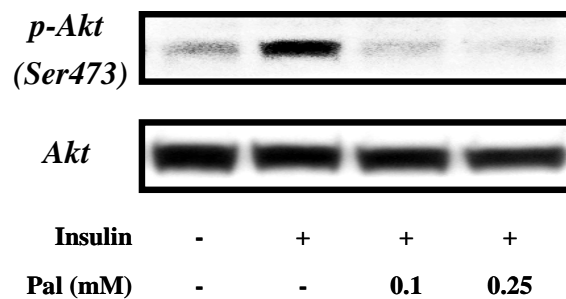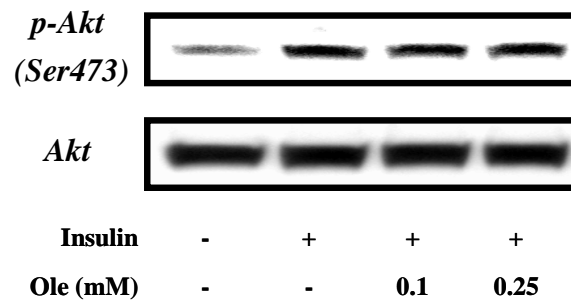
Supplemental Fig. 2. Effects of palmitate and oleate on expression levels of the SREBP-1c and IRS-2 genes in H4IIEC3 hepatocytes. H4IIEC3 cells were incubated in the presence or absence of palmitate (Pal) or oleate (Ole) for 16 h. Total RNA was extracted and subjected to reverse transcription. Using the cDNA as a template, the amounts of SREBP-1c and IRS-2 mRNA were detected by real-time PCR. The values are normalized to the level of 18S ribosomal RNA and expressed as mean fold increase over control ± S.E. (n = 3). ** $p < 0.01$, versus control.
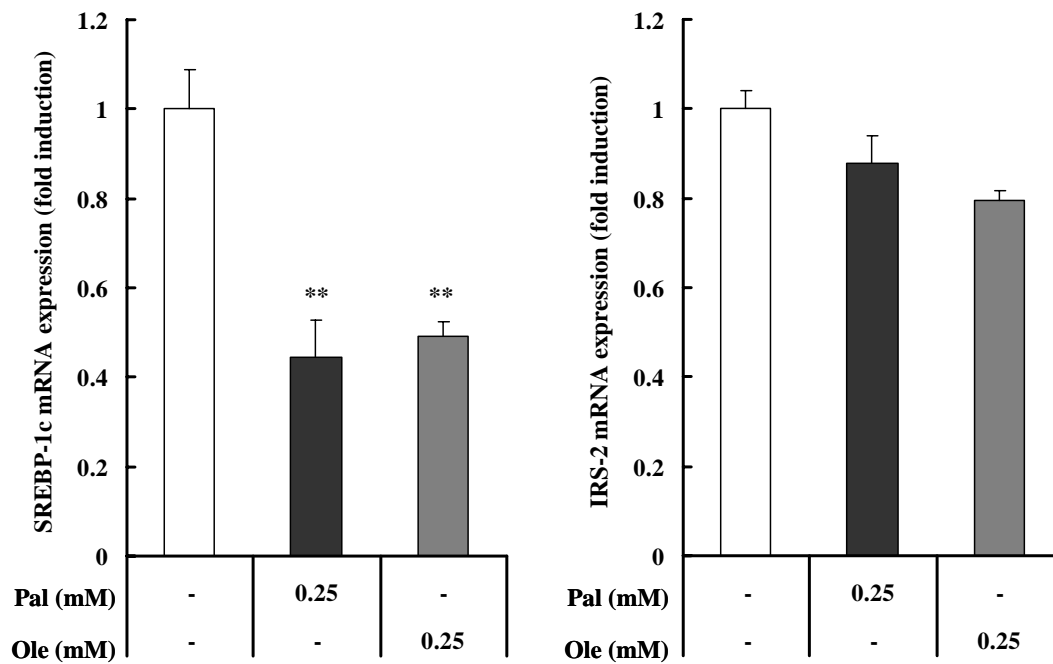
Supplemental Fig. 3. Effect of palmitate on ER stress in H4IIEC3 hepatocytes. H4IIEC3 cells were incubated in the presence or absence of palmitate (Pal) or the ER stress inducer tunicamycin (Tun) for 16 h. Total RNA was extracted and subjected to reverse transcription. Using the cDNA as a template, the amounts of GRP78 mRNA (A) or XBP-1 mRNA splicing (B) were detected by real-time PCR or reverse transcription PCR, respectively. (A) The values were normalized to the level of 18S ribosomal RNA and expressed as mean fold increase over control $\pm$ S.E. (n = 3). XBP-1u, unspliced XBP-1; XBP-1s, spliced XBP-1. ** $p < 0.01$, versus control.

(A)
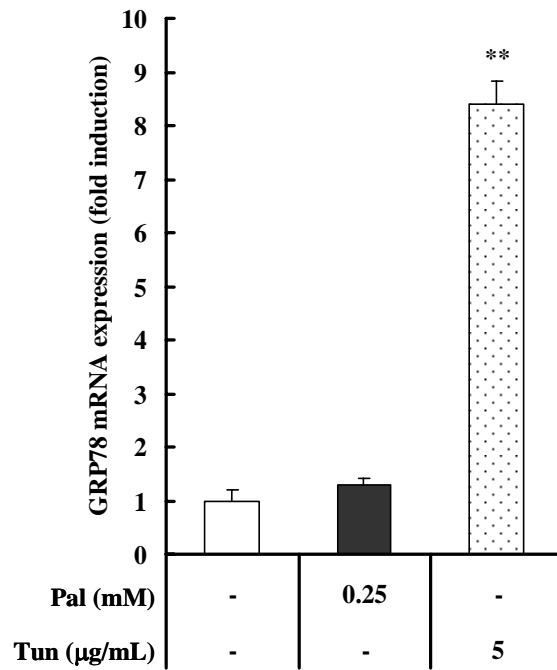
(B)
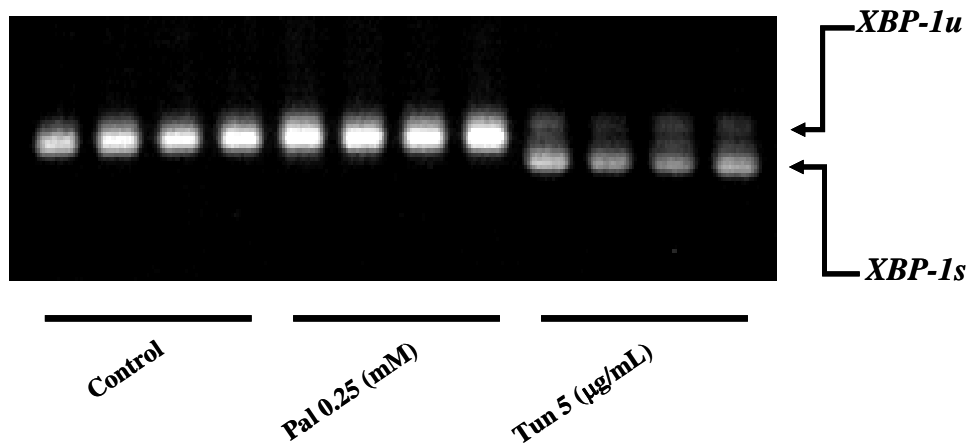
Supplemental Fig. 4. Comparison of insulin signaling with palmitate treatment and with the ER stress inducer tunicamycin in H4IIEC3 hepatocytes. (A) H4IIEC3 cells were incubated in the presence or absence of palmitate (Pal) or the ER stress inducer tunicamycin (Tun) for 16 h prior to stimulation with insulin (1 ng/mL, 15 min). Total cell lysates were resolved by SDS-PAGE, transferred to a PVDF membrane, and immunoblotted with the indicated antibodies. Detection was by enhanced chemiluminescence. Representative blots are shown. (B) The values from densitometry of four (p-Akt) or three (p-JNK) independent experiments are normalized to the level of total Akt or JNK protein, respectively, and expressed as the mean fold increase over control ± S.E. ** $p < 0.01$, versus insulin treatment alone. †† $p < 0.01$, versus control.
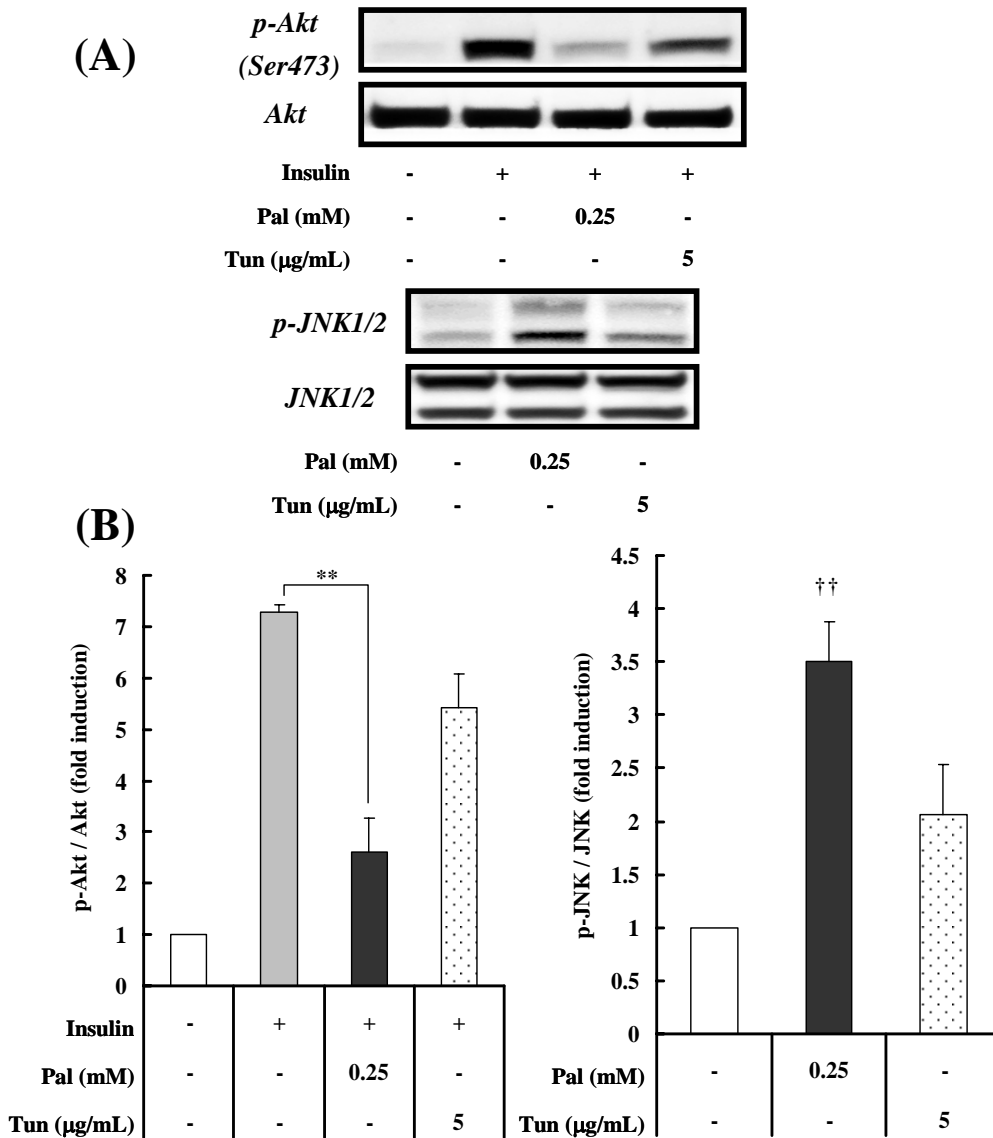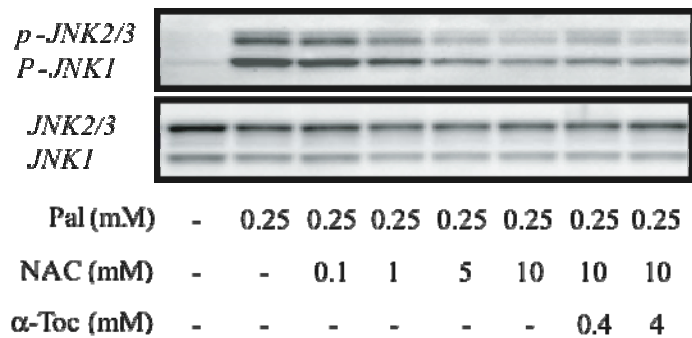
Supplemental Fig. 5. Restoration of intracellular GSH levels by N-acetyl-cysteine (NAC) in palmitate-treated H4IIEC hepatocytes. H4IIEC cells were incubated in the absence or presence of palmitate (Pal) and NAC for 16 h. Intracellular GSH levels were determined using a commercial kit (Total Glutathione Quantification Kit, DOJINDO). The values from three independent experiments were normalized to the level of total protein, respectively, and expressed as means ± S.E. (n = 3). * $P < 0.05$, ** $P < 0.01$, *** $P < 0.001$ versus control. † $P < 0.05$, †† $P < 0.01$ versus 0.25 mM Pal.
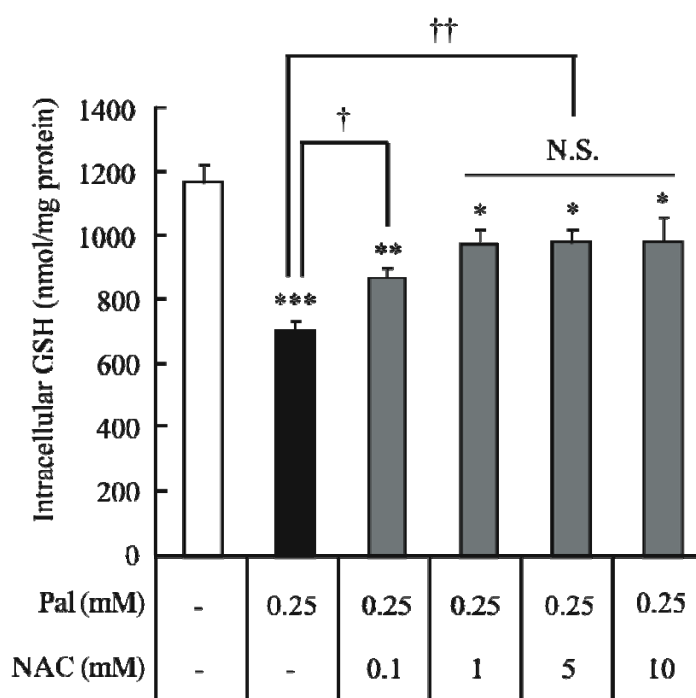
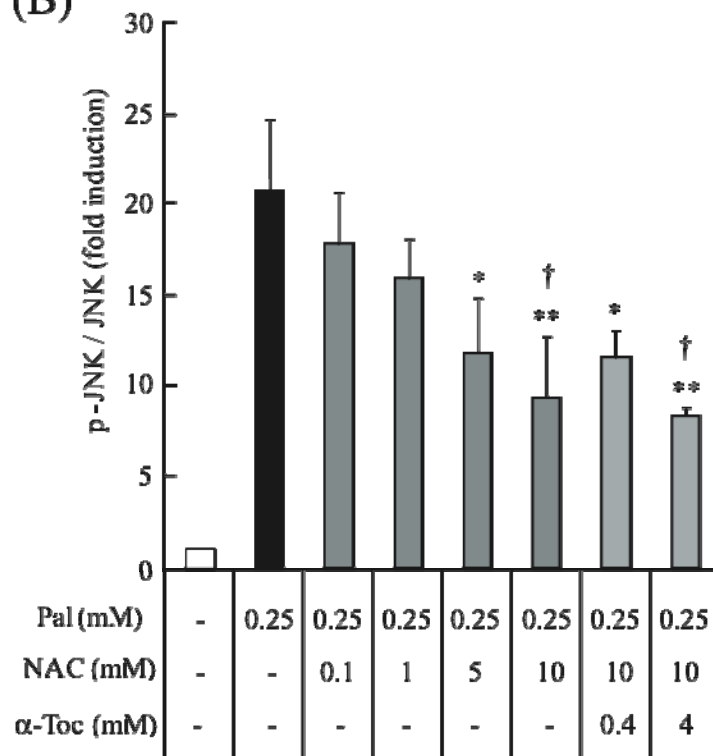Supplemental Fig. 6. N-acetyl-cysteine (NAC) and α-tocopherol (α-Toc) decrease palmitate-induced JNK activation in H4IIEC hepatocytes. (A) H4IIEC cells were incubated in the absence or presence of palmitate (Pal) and NAC and α-Toc for 16 prior to stimulation with insulin (1 ng/mL, 15 min). Total cell lysates were resolved by SDS-PAGE, transferred to a PVDF membrane, and immunoblotted with the indicated antibodies. Representative blots are shown. (B) The densitometric values from three independent p-JNK experiments were normalized to the level of total JNK and expressed as the mean fold increase over control ± S.E. * $P < 0.05$, ** $P < 0.01$ versus 0.25 mM Pal treatment. † $P < 0.05$ versus 0.25 mM Pal/0.1 mM NAC treatment.

Supplemental Fig. 7. N-acetyl-cysteine (NAC) and α-tocopherol (α-Toc) reverse palmitate-induced changes in insulin-stimulated Akt phosphorylation in H4IIEC hepatocytes. (A) H4IIEC cells were incubated in the absence or presence of palmitate (Pal) and NAC and α-Toc for 16 h prior to stimulation with insulin (1 ng/mL, 15 min). Proteins in total cell lysates were resolved by SDS-PAGE, transferred to a PVDF membrane, and immunoblotted with the indicated antibodies. Representative blots are shown. (B) The densitometric values from three independent p-Akt experiments were normalized to total Akt protein and expressed as the mean fold increase over control ± S.E. * $P < 0.05$, ** $P < 0.01$, *** $P < 0.001$ versus 0.25 mM Pal treatment.
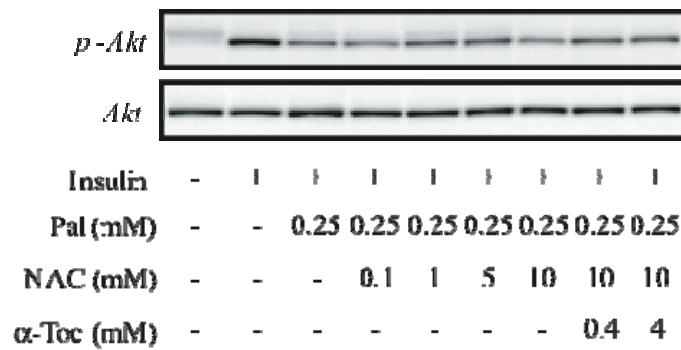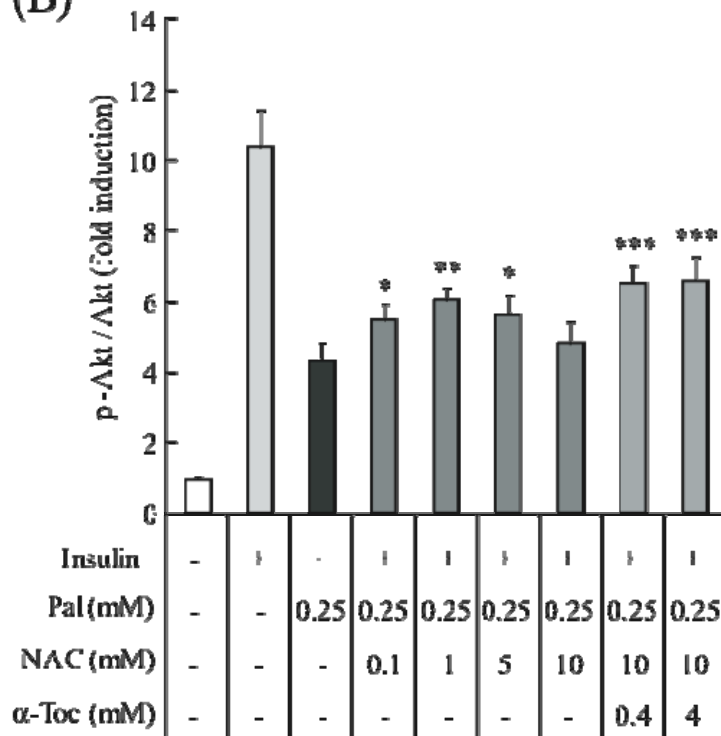
Supplemental Fig. 8. Effect of myriocin (Myr) on ceramide synthesis in H4IIEC hepatocytes. (A) H4IIEC cells were incubated in the absence or presence of palmitate (Pal) and Myr for 16 h. Ceramide was measured according to an established method (Araki et al., PNAS 94:11946, 1997). Signals were detected using a Typhoon 9400 Imager (GE Healthcare Bio-Sciences). Representative blots are shown. (B) The densitometric values from three independent experiments were normalized to the level of total protein and expressed as the mean fold increase over control ± S.E. * $P < 0.05$, *** $P < 0.001$ versus control. † $P < 0.05$ versus 0.25 mM Pal.
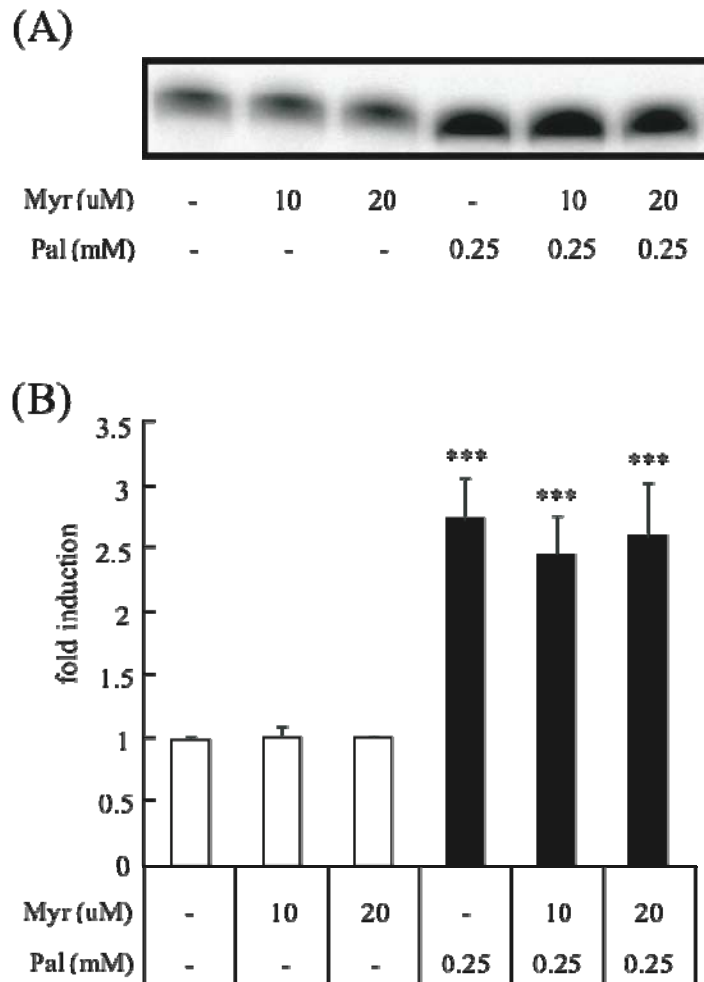
Figure 10